Geothermics 71 (2018) 306–319

Contents lists available at ScienceDirect

Geothermics

journal homepage: www.elsevier.com/locate/geothermics

Analysis of the impact of storage conditions on the thermal recovery efficiency of low-temperature ATES systems

Martin Bloemendal[a,b,*], Niels Hartog[b,c]

[a] Department of Water Management, Delft University of Technology, Delft, The Netherlands
[b] KWR, Watercycle Research Institute, Nieuwegein, The Netherlands
[c] Faculty of Geosciences, Utrecht University, Utrecht, The Netherlands

ARTICLE INFO

Keywords:
Aquifer Thermal Energy Storage (ATES)
Recovery efficiency
Well design
Storage conditions

ABSTRACT

Aquifer thermal energy storage (ATES) is a technology with worldwide potential to provide sustainable space heating and cooling using groundwater stored at different temperatures. The thermal recovery efficiency is one of the main parameters that determines the overall energy savings of ATES systems and is affected by storage specifics and site-specific hydrogeological conditions. Although beneficial for the optimization of ATES design, thus far a systematic analysis of how different principal factors affect thermal recovery efficiency is lacking. Therefore, analytical approaches were developed, extended and tested numerically to evaluate how the loss of stored thermal energy by conduction, dispersion and displacement by ambient groundwater flow affect thermal recovery efficiency under different storage conditions. The practical framework provided in this study is valid for the wide range of practical conditions as derived from 331 low-temperature (< 25 °C) ATES systems in practice.

Results show that thermal energy losses from the stored volume by conduction across the boundaries of the stored volume dominate those by dispersion for all practical storage conditions evaluated. In addition to conduction, the displacement of stored thermal volumes by ambient groundwater flow is also an important process controlling the thermal recovery efficiencies of ATES systems. An analytical expression was derived to describe the thermal recovery efficiency as a function of the ratio of the thermal radius of the stored volume over ambient groundwater flow velocity (R_{th}/u). For the heat losses by conduction, simulation results showed that the thermal recovery efficiency decreases linearly with increasing surface area over volume ratios for the stored volume (A/V), as was confirmed by the derivation of A/V-ratios for previous ATES studies. In the presence of ambient groundwater flow, the simulations showed that for $R_{th}/u < 1$ year, displacement losses dominated conduction losses. Finally, for the optimization of overall thermal recovery efficiency as affected by these two main processes, the optimal design value for the ratio of well screen length over thermal radius (L/R_{th}) was shown to decrease with increasing ambient flow velocities while the sensitivity for this value increased. While in the absence of ambient flow a relatively broad optimum exists around an L/R_{th}-ratio of 0.5–3, at 40 m/year of ambient groundwater flow the optimal L/R_{th}-value ranges from 0.25 to 0.75. With the insights from this study, the consideration of storage volumes, the selection of suitable aquifer sections and well screen lengths can be supported in the optimization of ATES systems world-wide.

1. Introduction

World-wide efforts aim to reduce greenhouse gas emissions and to meet energy demands sustainably (EU, 2010; SER, 2013; UN, 2015). Global demand for heating and cooling in the built environment accounts for about 40% of the total energy consumption (EIA, 2009; Kim et al., 2010; RHC, 2013). In reducing this demand, the use of Aquifer Thermal Energy Storage[1] (ATES) systems for space heating and cooling has a high potential in the many regions worldwide that have substantial seasonal, or sometimes diurnal, variations in ambient air temperature combined with favorable geohydrological conditions (Bloemendal et al., 2015).

Although much of the early ATES research has focused on storage at high temperatures (Molz et al., 1983, 1978; Nagano et al., 2002; Réveillère et al., 2013; Tsang, 1978), most practical experience with seasonal ATES systems has in recent years been gained in particularly

* Corresponding author at: Delft University of Technology, Department of Water Management, PO Box 5048, 2600 GA, Delft, The Netherlands.
E-mail address: j.m.bloemendal@tudelft.nl (M. Bloemendal).

[1] Also often referred to as open loop geothermal storage systems. Closed loop or borehole heat exchangers also have a high potential for energy savings. In this paper the focus is on ATES systems because they provides a more (cost) effective option for large scale cooling and heating in urban areas mainly for utility buildings and large scale housing complexes.

http://dx.doi.org/10.1016/j.geothermics.2017.10.009
Received 14 June 2017; Received in revised form 9 September 2017; Accepted 17 October 2017

Nomenclature

A	Surface area of the heat storage in the aquifer [m^2]
α	Dispersivity [m]
c_w	Volumetric heat capacity of water; 4.2 × 10^6 [$J/m^3/K$]
c_{aq}	Volumetric heat capacity of saturated porous medium; 2.8 × 10^6 [$J/m^3/K$]
D_{eff}	Effective dispersion [m^2/d]
D_T	Thermal dispersion [m^2/d]
$\Delta\overline{T}$	Average temperature difference between warm and cold well [°C]
E	Energy [J]
η_{th}	Thermal efficiency [−]
i	Groundwater head gradient [−]
k	Hydraulic conductivity [m/d]
k_{Taq}	Thermal conductivity of water and particles; 2.55 [W/m/K]
L	Well screen length [m]
n	Porosity; 0.3 [−]
Q	Pumping rate of ATES wells [m^3/d]
ρ	Water density; 1000 [kg/m^3]
R	Thermal Retardation factor [−]
R_{th}	Thermal radius [m]
R_h	Hydraulic radius [m]
τ	Dimensionless time of travel parameter [−]
t_{sp}	Length of storage period [d]
T	Temperature [°K]
t	Time step [d]
u	Ambient groundwater flow velocity [m/d]
v	Flow velocity of the groundwater [m/d]
u_*	Velocity of the thermal front [m/d]
V	Yearly (permitted or actual) storage volume groundwater [m^3]

several European countries (Eugster and Sanner, 2007; Fry, 2009; Haehnlein et al., 2010; Willemsen, 2016). These ATES systems seasonally store thermal energy at relatively low temperatures (< 25 °C) alternating between cooling and, assisted by a heat pump, heating mode (Fig. 1). The number of ATES systems has grown rapidly in the past decade particularly in The Netherlands (Fig. 2), a country with a moderate climate and widespread presence of thick sedimentary aquifers. The introduction of progressively stricter energy efficiency requirements for buildings (Energy Performance Coefficient (EPC)), stimulated the adoption of ATES in the built environment. As a result, there are currently almost 2000 systems in operation in relatively shallow sandy aquifers (typically 20–150 m.b.g.l.).

For both an optimal energy performance of an ATES system as well as minimal effect on the subsurface, the thermal energy recovery efficiency needs to be as high as possible. Under these conditions, the electricity required for groundwater pumping and heat pump (Fig. 1) is minimized.

Previous studies have shown that the thermal recovery efficiency of ATES systems are negatively affected by thermal energy losses from the stored volume by conduction, diffusion and dispersion (Doughty et al., 1982; Sommer et al., 2014). While for high temperature (> 45 °C) ATES systems, the negative impact of the buoyancy of the stored hot water on thermal recovery efficiency typically needs to be considered (Lopik et al., 2016; Zeghici et al., 2015), this can be neglected for low temperature ATES systems (Doughty et al., 1982; Zuurbier et al., 2013). However, as these low temperature ATES systems are typically targeting relatively shallow aquifers, the impact of stored volume displacement by ambient groundwater flow requires consideration. Although the impact of ambient groundwater flow on injected and recovered water volumes has been studied (Bear and Jacobs, 1965; Ceric and Haitjema, 2005), the impact of ambient groundwater flow on thermal recovery efficiency in ATES systems, has thus far not been explored. Moreover, it is unclear how the combined impact of these processes (dispersion, conduction and advection) affects the thermal recovery efficiency of ATES systems under practical conditions and how the efficiency can be optimized.

Therefore, the aim of this study is to use analytical methods to elucidate the impact of ambient groundwater flow and conduction and dispersion on the thermal recovery efficiency of ATES systems and to use numerical methods to assess how the combined heat loss by multiple processes can be minimized. As a practical framework for the conditions investigated, the wide range of ATES system characteristics and hydrogeological conditions in the Netherlands was used. The resulting insights are meant to provide a useful basis to enable the optimization of the thermal recovery efficiency of ATES systems and to further optimize development for sustainable heating and cooling of buildings world-wide.

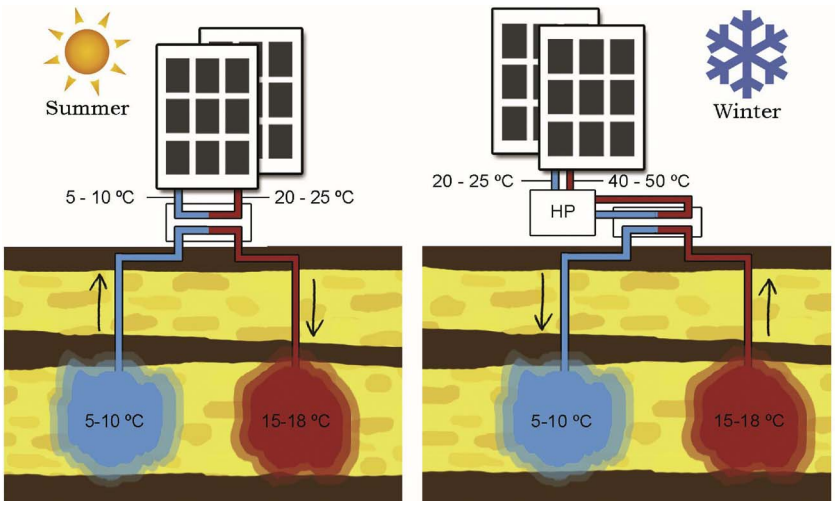

Fig. 1. Illustration of the basic working principle of a low-temperature seasonal ATES system. Left: in direct cooling mode while storing heat for winter. Right: vice-versa in heating mode supported by a heat pump while storing cooling capacity for summer.

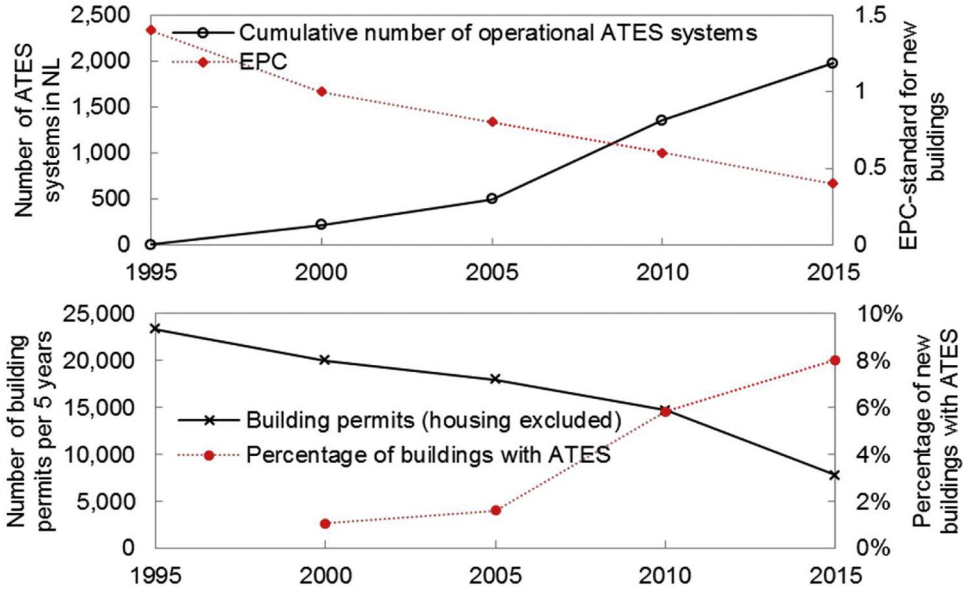

Fig. 2. Top: increase of number of ATES systems during recent years in the Netherlands along with the decreasing EPC-standard for dwellings, The EPC value is a normalized value of the expected energy use of a building (CBS, 2016a; LGR, 2012; Ministry-of-Internal-Affairs, 2012). Bottom: The increasing percentage of new buildings build with ATES system (CBS, 2016a,b).

2. Materials and methods

2.1. Theory of heat transport and recovery during ATES

2.1.1. Definition of thermal recovery efficiency for ATES systems

The thermal energy stored in an ATES system can have a positive and negative temperature difference between the infiltrated water and the surrounding ambient groundwater, for either heating or cooling purposes (Fig. 1). In this study the thermal energy stored is referred to as heat or thermal energy; however, all the results discussed equally apply to storage of cold water used for cooling. As in other ATES studies (Doughty et al., 1982; Sommer, 2015), the recovery efficiency (η_{th}) of an ATES well is defined as the amount of injected thermal energy that is recovered after the injected volume has been extracted. For this ratio between extracted and infiltrated thermal energy (E_{out}/E_{in}), the total infiltrated and extracted thermal energy is calculated as the cumulated product of the infiltrated and extracted volume with the difference of infiltration and extraction temperatures ($\Delta T = T_{in} - T_{out}$) for a given time horizon (which is usually one or multiple storage cycles), as described by:

$$\eta_{th} = \frac{E_{out}}{E_{in}} = \frac{\int \Delta T\, Q_{out}\, dt}{\int \Delta T\, Q_{in}\, dt} = \frac{\Delta \overline{T}_{out} V_{out}}{\Delta \overline{T}_{in} V_{in}}, \quad (1)$$

with, Q being the well discharge during time step t and $\Delta\overline{T}$ the weighted average temperature difference between extraction and injection. Injected thermal energy that is lost beyond the volume to be extracted is considered lost as it will not be recovered. To allow unambiguous comparison of the results the simulations in this study are carried out with constant yearly storage and extraction volumes ($V_{in} = V_{out}$).

2.1.2. Loss of heat due to displacement by ambient groundwater flow

Significant ambient groundwater flow is known to occur at ATES sites (Bonte et al., 2013b; Groot, 2013; Hartog et al., 2013), which leads to displacement of the injected volumes (Bear and Jacobs, 1965; Bonte et al., 2013a). This may lead to significant reduction in the thermal energy recovery efficiency of ATES systems as ambient groundwater flow (u) contributes to thermal losses by displacing the injected water during storage. The heat transport velocity (u_*) is retarded with respect to ambient groundwater flow (Doughty et al., 1982; Hecht-Mendez et al., 2010) due to heat storage in the aquifer solids. The thermal retardation (R) depends on porosity (n) and the ratio between volumetric heat capacities of water (c_w) and aquifer (c_{aq}, with $c_{aq} = nc_w + (1 - n)c_s$ and c_s the solids volumetric heat capacity), following:

$$u_* = \frac{1}{R}u = \frac{nc_w}{c_{aq}}u \approx 0.5 \cdot u. \quad (2)$$

Resulting in a heat transport velocity at approximately 50% of the groundwater flow velocity (u). Under conditions of ambient groundwater flow, thermal energy stored in an aquifer will thus be displaced and can only be partly (Bear and Jacobs, 1965) recovered.

2.1.3. Loss of heat by dispersion and conduction

Mechanical dispersion and heat conduction spread the heat over the boundary of the cold and warm water bodies around the ATES wells. As a consequence of the seasonal operation schedule, diffusion losses are

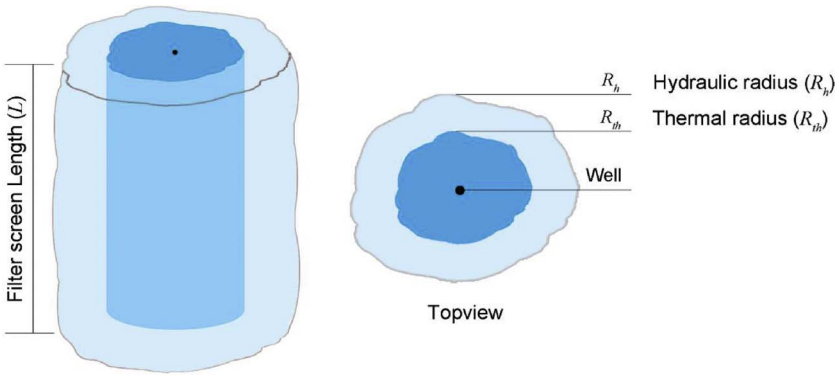

Fig. 3. Simplified presentation of the resulting subsurface thermal and hydrological storage cylinder for an ATES system for homogeneous aquifer conditions.

Table 1
MODFLOW simulation parameter values (Caljé, 2010; Hecht-Mendez et al., 2010).

Parameter	value
Horizontal conductivity aquifers	25 m/d
Horizontal conductivity aquitards	0.05 m/d
Longitudinal dispersion	1 m
Transversal dispersion	0,1 m
Bulk density	1890 kg/m^3
Bulk thermal diffusivity	0.16 m^2/day
Solid heat capacity	880 J/kg °C
Thermal conductivity of aquifer	2.55 W/m °C
Effective molecular diffusion	$1{\cdot}10^{-10}$ m^2/day
Thermal distribution coefficient	$2{\cdot}10^{-4}$ m^3/kg

negligible (Anderson, 2005; Bear, 1979). Both other processes are described by the effective thermal dispersion (D_{eff}) which illustrates the relative contribution of both processes to the losses, following:

$$D_{eff} = \frac{\kappa_{Taq}}{nc_w} + \alpha\frac{v}{n}, \tag{3}$$

where, the first term represents the conduction, which depends on the volumetric heat capacity (c_w) of water and the thermal conductivity (k_{Taq}) and porosity (n) of the aquifer material which are considered to remain constant at about 0.15 [m^2/d] in a sandy aquifer with porosity of 0.3. The rate at which conduction occurs can be determined by the increasing standard deviation: $\sigma = \sqrt{2D_T t}$, with D_T, the effective thermal dispersion (the left hand term of Eq. (3) and t the storage time). For half a year storage period the rate at which heat moves through conduction is about 7 m.

The second term of Eq. (3) represents the mechanical dispersion, which depends on the dispersivity (α) of the subsurface, porosity and the flow velocity of the water (v), which is the sum of the force convection due to the infiltration and extraction of the well, as well as the ambient groundwater flow (u). For ATES wells that fully penetrate an aquifer confined by aquitards, the dispersion to cap and bottom of the thermal cylinder (Fig. 3) is negligible due to the lack of flow (Caljé, 2010; Doughty et al., 1982). With regularly applied values of 0.5–5 for the dispersivity (Gelhar et al., 1992), the dispersion is in the same order of magnitude as the conduction at flow velocities of 0.01–0.1 m/d.

Since losses due to mechanical dispersion and conduction occur at the boundary of the stored body of thermal energy, the thermal recovery efficiency therefore depends on the geometric shape of the thermal volume in the aquifer (Doughty et al., 1982). Following Doughty et al. (1982), the infiltrated volume is simplified as a cylinder with a hydraulic radius (R_h) defined as:

$$R_h = \sqrt{\frac{V_{in}}{n\pi L}} \tag{4}$$

and for which the thermal radius (R_{th}) is defined as:

$$R_{th} = \sqrt{\frac{c_w V_{in}}{c_{aq}\pi L}} = \sqrt{\frac{nc_w}{c_{aq}}}R_h = \sqrt{\frac{1}{R}}R_h \approx 0.66{\cdot}R_h. \tag{5}$$

The size of the thermal cylinder thus depends on the storage volume (V), screen length (L, for a fully screened aquifer), porosity (n) and water and aquifer heat capacity (Fig. 3). This equation is approximate because heterogeneities and partially penetration of the screens are ignored. Doughty et al. (1982) introduced a dimensionless ratio of screen length and the thermal radius (L/R_{th}) as a parameter to describe thermal recovery efficiency of ATES systems for a particular stored thermal volume. They found that the ATES recovery efficiency has a flat optimum between a value of 1and 4 for this ratio.

Losses due to interaction between ATES systems are not taken into account in this research. Also interaction between the warm and cold well of the same system is not taken into account as this is prevented by the permitting requirement to ensure sufficient separation distance (three times the thermal radius).

2.2. Numerical modeling of ATES

As losses due to conduction, dispersion and displacement occur simultaneously, MODFLOW (Harbaugh et al., 2000) simulations is used to evaluate their combined effect on recovery efficiency. For the simulation of ambient groundwater flow and heat transport under various ATES conditions, a geohydrological MODFLOW model (Harbaugh et al., 2000) coupled to the transport code MT3DMS (Hecht-Mendez et al., 2010; Zheng and Wang, 1999). These model codes use finite differences methods to solve the groundwater and (heat) transport equations. This allows for simulation of infiltration and extraction of groundwater in and from groundwater wells and groundwater temperature distribution, as was done in previous ATES studies e.g. (Bonte, 2013; Caljé, 2010; Sommer, 2015; Visser et al., 2015). In the different modeling scenarios the storage volume is varied between 12,000 and 300,000 m^3 with flow rates proportionally ranging from 8 to 200 m^3/h, screen lengths between 10 and 105 m and ambient groundwater flow velocities between 0 and 50 m/y following the characteristics from Dutch practice as will be introduced in the next section. Density differences are neglected as this is considered a valid assumption (Caljé, 2010) for the considered ATES systems that operate within a limited temperature range (< 25 °C). The parameter values of the model are given in Table 1, the following discretization was used:

- Model layers; the storage aquifer is confined by two 10 m thick clay layers. The storage aquifer is divided in 3 layers, a 5 m thick upper and lower layer, the middle layers' thickness is changed according to the required screen length of the modeled scenario.
- The spatial discretization used in horizontal direction is 5 × 5 m at well location, gradually increasing to 100 × 100 m at the borders of the model. A sufficiently large model domain size of 6 × 6 km was used to prevent boundary conditions affecting (< 1%) simulation results. The gradually increasing cell size with distance from the wells results the cell size of 15 m at 200 m of the well. This discretization is well within the minimum level of detail to model the temperature field around ATES wells as was identified by Sommer et al. (2014).
- A temporal discretization of one week is used, which is sufficiently small to take account for the seasonal operation pattern and resulting in a courant number smaller than 0.5 within the area around the wells where the process we care about occur. The simulation has a horizon of 10 years, sufficiently long to achieve stabilized yearly recovery efficiencies.

The PCG2 package is used for solving the groundwater flow, and the MOC for the advection package simulating the heat with a courant number of 1. To set the desired ambient groundwater flow velocity for the different scenarios simulated, the constant hydraulic head boundaries were used to set the required hydraulic gradient. In the aquifer an ATES doublet is placed with a well distance of five times the maximum thermal radius of the wells to avoid mutual interaction between the warm and cold storage volumes. In scenarios with groundwater flow, the ATES wells are oriented perpendicular to the flow direction.

The energy demand profile of ATES systems varies due to variations in weather conditions and building use which is of importance for the actual value of the thermal efficiency. For 12 varying scenarios the efficiencies are determined for both a weather dependent and the regular energy demand profile, showing that the efficiencies of the corresponding conditions differ. However, they show the same relation according to the changes in conditions; the Pearson correlation coefficient of the two simulation result collections is 0,97. Based on this evaluation all simulations are done with one basic energy demand profile, to allow for comparison with the analytical solutions also the constant storage volume energy demand pattern will be used; heat injection, storage,

extraction and again storage during 13 weeks each as is commonly done in other ATES research (e.g. (Sommer et al., 2014; Zuurbier et al., 2013)).

2.3. Characteristics and conditions of ATES systems in The Netherlands

2.3.1. Characteristics of the ATES systems

Data on the location, permitted yearly storage volume, pump capacity and screen length of 331 ATES systems in The Netherlands (15% of total number of systems) were obtained from provincial databases that keep combined records for ATES characteristics of interest for this research (Provinces of Gelderland, Noord-Brabant, Noord-Holland, Utrecht and Drenthe, Fig. 4).

2.3.2. Geohydrological conditions at ATES systems

For a geographically representative subset of 204 ATES systems (Fig. 4) it was possible to extract available aquifer thickness and derive estimates on the ambient groundwater flow, as this additional data are not available in the provincial databases. These estimates are based on hydraulic conductivity and head gradients derived from the Dutch geologic databases (TNO, 2002a) for the coordinates of these ATES systems. The groundwater head gradient is read from equipotential maps (TNO, 2002a) while the hydraulic conductivity and aquifer thickness is obtained from local soil profiles in the REGIS II (TNO, 2002a,b) subsurface model of the Netherlands and literature values for hydraulic conductivity (Bear, 1979; Kasenow, 2002) corresponding to the soil profiles from the bore logs. The data are abstracted and processed for the aquifer regionally targeted for ATES systems, therefore, ATES systems with wells installed in other aquifers are excluded from the local analysis. Legal boundaries are also taken into account, in Noord-Brabant for instance it is not allowed to install ATES systems deeper than 80 m below surface level, so any aquifer available below 80 m is disregarded for the systems in this province. For all locations a porosity value of 30% is assumed, a value common for Dutch sandy aquifers (Bloemendal et al., 2015; NVOE, 2006; SIKB, 2015a).

3. Results

3.1. ATES system properties in The Netherlands

3.1.1. Permitted capacity and screen length

The permitted capacity of the ATES systems ranges up to 5,000,000 m^3/year but most (~70%) are smaller than 500,000 m^3/year (Fig. 5, Table 2). The observed differences in ATES system characteristics for the different provinces were limited and therefore not presented separately.

To be able to evaluate the resulting geometry of the storage volume in evaluating dispersion and conduction losses it is assumed that the

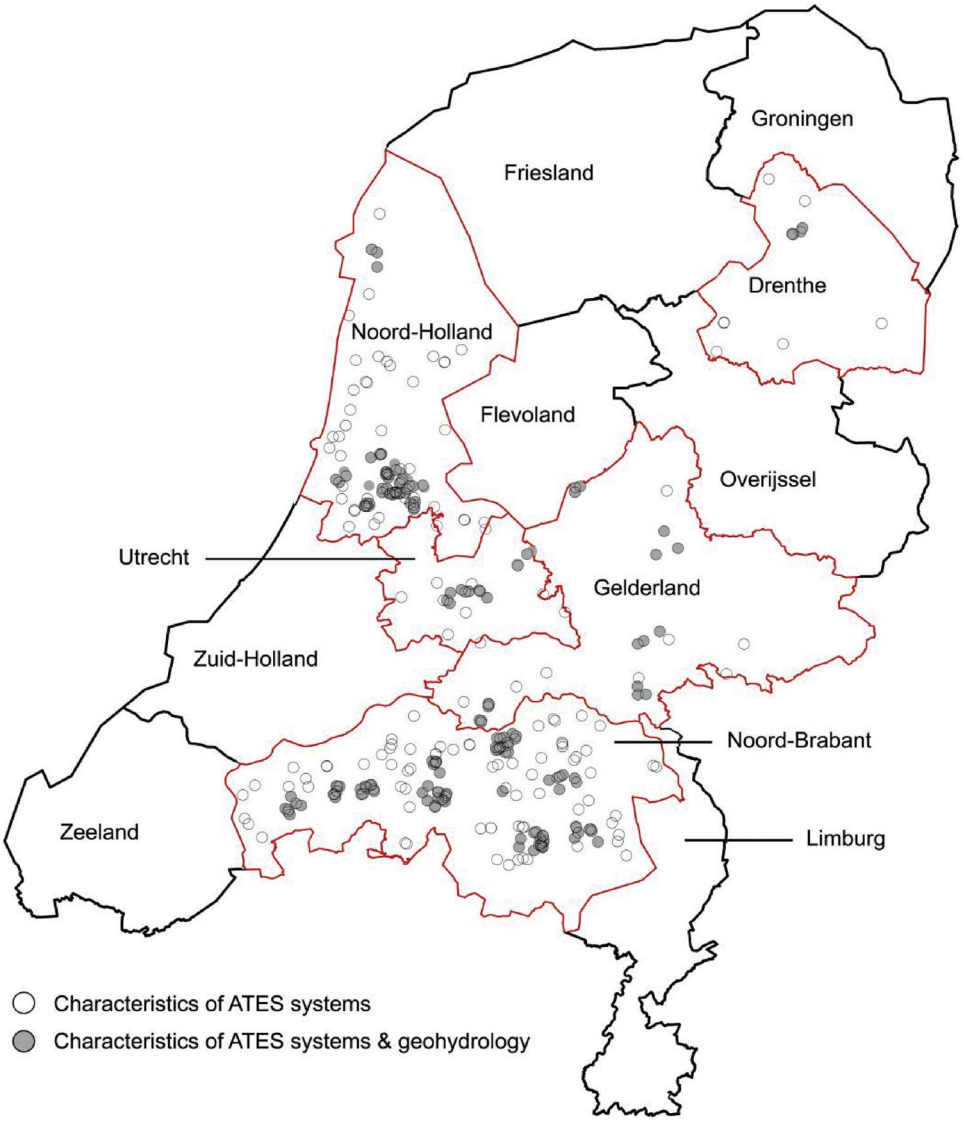

Fig. 4. Locations of selected ATES systems from 5 provincial databases. Other provinces have ATES systems as well but in their databases some characteristics required for this evaluation were missing, Open circles indicate locations for which ATES characteristics were available. Filled circles indicate locations for which also the local geohydrological conditions were available.

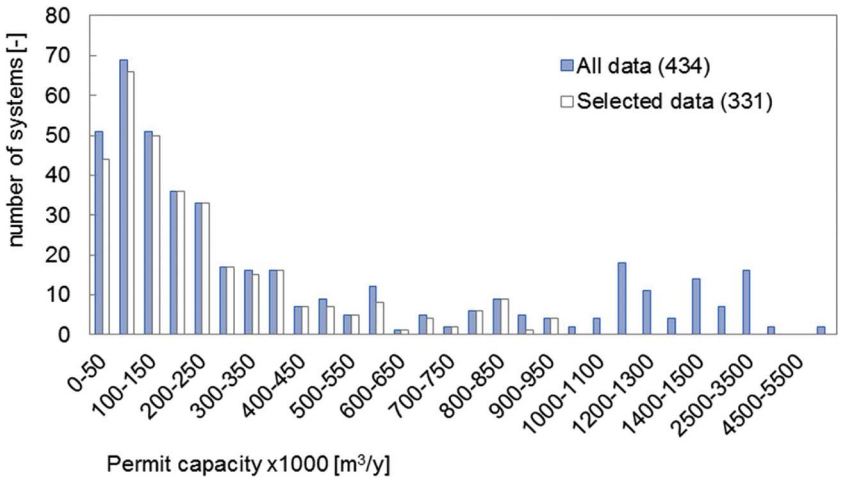

Fig. 5. Frequency distribution of dataset according to permitted yearly storage volume of groundwater. Distribution of well design metrics of selected data is shown separately.

Table 2
ATES system characteristics in provincial datasets selected for this study.

	Number of ATES systems	Permitted capacity (*V*) *[m^3/y]*			Installed screen length (*L*) *[m]*		
		0.25 perc.	Average	0.75 perc.	0.25 perc.	Average	0.75 perc.
Initial data	434	90,000	539,000	674,000	20	37	45
selected data	331	80,000	244,000	320,000	20	32	40

thermal energy is stored in a single cylindrical volume. Most ATES systems in the Netherlands are single doublet systems or multiple doublet systems with clustered warm and cold wells. However, particularly for some larger systems, warm and cold wells are not clustered, due to for example spatial planning or geohydrological and/or geotechnical reasons (Bloemendal et al., 2015). Unfortunately the provincial data did not include the number or type of well pairs. Therefore the data was filtered for the systems for which a multiple number of well pairs or other deviating aspects could be confirmed. Those systems mostly belong to the largest 10% of the systems, or belong to outliers in the data distribution of screen length over stored volume, and were therefore excluded. For the largest systems, multiple doublets were confirmed for several systems (e.g. C, D, F, G, H, I). In addition, some errors were found in the data of the provincial databases, inconsistent, incomplete entries (e.g. E) with errors (e.g. impossible short or long screen lengths), such as monowell systems with only one very long screen which should be divided in two screens (A and B in Fig. 6). As a result of this validation of the dataset, 331 systems were selected for further evaluation (Fig. 6). The data used for analysis represents about 15% of the approximately 2000 systems operational in the Netherlands (Willemsen, 2016).

3.1.2. Geohydrological conditions

Table 3 shows the overall geohydrological characteristics at the location of 204 ATES systems. Both hydraulic conductivity and ambient groundwater flow velocity show a wide range.

3.2. Analytical evaluation of ATES thermal recovery

3.2.1. Loss of thermal energy due to dispersion and conduction

Both conduction and dispersion losses occur at the boundary of the stored thermal cylinder. Following Eq. (3); near the well, where flow velocity of the infiltrated water (*v*) is high, dispersion dominates the conduction term, while further from the well, the effects of dispersion decreases. Eq. (3) and the values for the dispersion and aquifer properties in Table 1 are now used to identify the distance from the well at

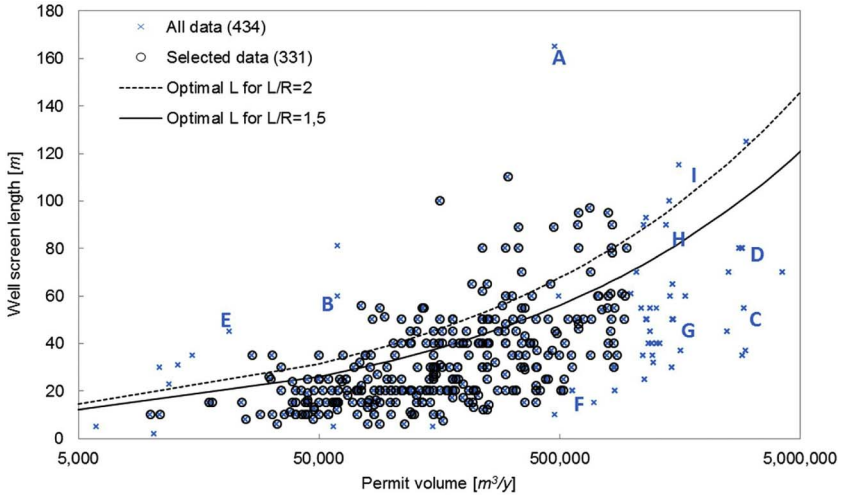

Fig. 6. Dataset characteristics; outliers are excluded from the dataset. A, B = monowells with only top of upper and bottom of lower filter in the data, C = University Campus ~6 doublets, D = Office with 3 doublets, E = Office building with only extracted volume of one year available in data, unrealistically small for size of building, F = office with 4 doublets, G = Hospital with 4 doublets, H = conference center with 2 monowells, I = Office with 3 doublets.

Table 3
Ranges in geohydrological characteristics of the 204 ATES systems under consideration, for which geohydrological conditions could be retrieved.

Available aquifer thickness range [m]	Hydraulic conductivity Range [m/d]	Groundwater flow range [m/y]
30–180	5–45	3–100

which the dominating process contributing to loss, changes from dispersion to conduction, Fig. 7. The pump capacity data of the ATES systems together with the storage volume and screen length are used to plot the thermal radii of the systems with respect to their maximum specific discharge, showing that even assuming a relatively high dispersivity of 5 m, beyond 10% of permitted storage volume infiltration, conduction is dominating in the dispersivity equation, indicating that at full storage capacity conduction losses will be dominating.

When the infiltration continues, the movement of the thermal front is dominated by the advective heat transport of the injection., The (high) dispersion losses that occur at the high flow velocities close to the well are "overtaken" when infiltration of heat continues, resulting in sharp heat interface as the infiltration volume increases. This sharp interface remains sharp during infiltration because the heat injected by the well travels faster than the standard deviation for the conduction ($\sigma = \sqrt{2D_T t}$). During storage and extraction the interface will become less sharp due to respectively conduction and the opposite effect of these mechanisms. The heat that thus stays behind causes that efficiency improves and stabilizes over multiple storage cycles. From which it is concluded that losses can be minimized by minimizing the total surface area of the circumference and the cap and bottom of the thermal cylinder (A) of the stored heat volume (V) in the aquifer. This can be done by identifying an appropriate screen length according to the required storage volume and local conditions, in order to minimize the surface area − volume ratio;

$$\frac{A}{V} = \frac{2\pi R_{th}^2 + 2\pi R_{th} L}{\pi R_{th}^2 L} = \frac{2}{L} + \frac{2}{R_{th}}. \quad (6)$$

For any given storage volume an optimal screen length exists at which conduction and dispersion losses are minimal at the screen length − thermal radius ratio (L/R_{th}) is 2, when the diameter of the cylindrical storage volume is equal to its screen length. From Fig. 8 can be seen that for larger storage volumes the A/V-ratio is smaller, and less sensitive at larger screen lengths, exhibiting a relatively flat minimum compared to small storage volumes. Although the absolute losses increase with increasing storage volume, the relative losses are smaller.

To identify the optimal screen length the derivative for surface area of the thermal cylinder is equated to zero, which results in an expression for optimal screen length as a function of required storage volume;

$$A = 2\frac{c_w V}{c_a L} + 2\pi\sqrt{\frac{c_w V}{\pi c_a L}}L \rightarrow A' = \frac{-2\pi c_w V}{c_a L^2} + \pi\sqrt{\frac{c_w V}{\pi c_a}}\frac{1}{\sqrt{L}} \rightarrow L \approx 1.23 \cdot \sqrt[3]{V}. \quad (7)$$

Consequently, relatively small storage volumes experience higher losses due to dispersion losses. Because there is no or little flow to and from the confining layers of an ATES well, conduction losses along the interface with the confining soil layers may differ from the ones around the circumference. Therefore Doughty et al. (1982) distinguished between the two in their research to optimize well design, to account for the reduced conduction losses to confining layers after several storage cycles. Their Simulation showed that efficiency increases with the first number of storage cycles and found that the optimal ratio between screen length and thermal radius (L/R_{th}) has a flat optimum around 1.5 when taking into account different thermodynamic properties of aquifers and aquitards. Substituting the expression for the thermal radius (R_{th}, Eq. (5)) in the optimal relation of $L/R_{th} = 1.5$ gives the optimal screen length (L) as a function of storage volume (V);

$$L = \sqrt[3]{\frac{2.25 c_w V}{c_a \pi}} \approx 1.02 \cdot \sqrt[3]{V}. \quad (8)$$

This shows that the solution for the screen length results in the same third root of the storage volume, only with a smaller constant 1.02 [−] instead of 1.23 [−] as was derived from the optimal A/V-ratio solution, Eq. (7) & (8). This is the case because over multiple cycles, the conduction losses to "cap & bottom" decrease; losses from earlier cycles dampen the losses during following cycles.

From the lines for L/R_{th} is 1.5 it can be seen that on average, screen lengths are designed far from optimal with respect to minimizing conduction losses. Doughty et al. (1982) however, found a flat optimum for L/R_{th}-value, thus it may also be acceptable when the L/R_{th}-value is between 1 and 4, based on the moment of deflection of the L/R_{th}-curve constructed by Doughty et al. (1982). However most systems have L/R_{th}-values lower than 1, indicating that screen lengths used in Dutch practice are relatively short (Fig. 9). Analysis shows that 56% of the ATES systems with an $L/R_{th} < 1$ have insufficient aquifer thickness available for longer screens.

3.2.2. The effect of ambient groundwater flow on recovery efficiency

For the analysis of the impact of ambient groundwater flow on the recovery efficiency, it is assumed that a cylindrical shape of the injected volume is maintained during displacement. Ceric and Haitjema (2005) determined that this assumption is valid for conditions where their dimensionless time of travel parameter τ, (Ceric and Haitjema, 2005) is smaller than one;

$$\tau = \frac{2\pi (ki)^2 L t_{sp}}{nQ} = \frac{2\pi n u^2 L t_{sp}}{Q}. \quad (9)$$

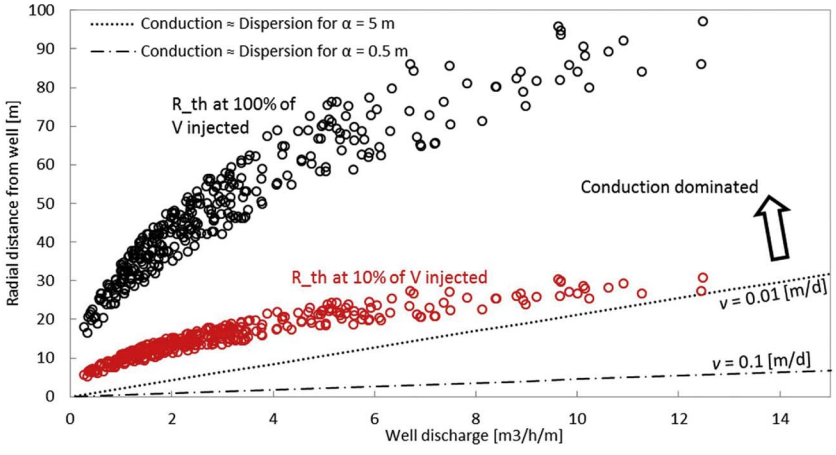

Fig. 7. Lines: the relation between specific well discharge and radial distance at which the radial flow velocities where conduction and dispersion are equal (Eq. (3)) for the outer-bounds of the range of thermal dispersivity regularly applied in literature. Open circles the thermal front of the ATES systems in the data at different storage capacities related to their specific well discharge.

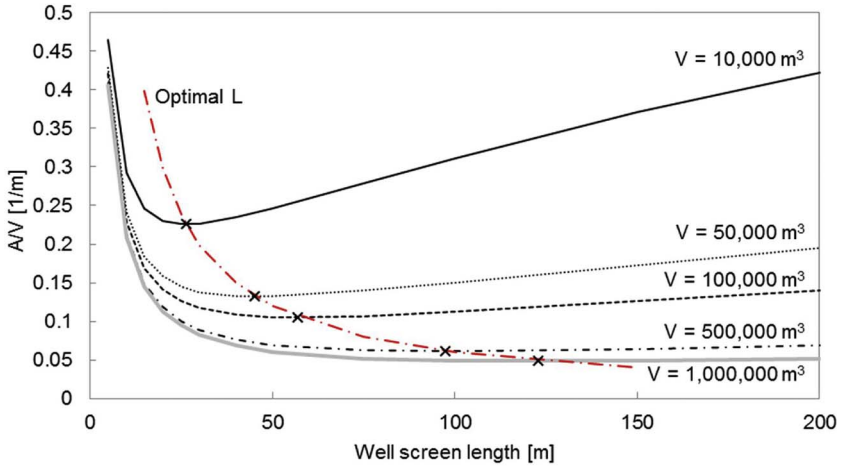

Fig. 8. The A/V values for different storage volumes and well screen lengths.

The groundwater head gradient (i), hydraulic conductivity (k), screen length (L) and pumping rate (Q) of the ATES systems in the data are used to determine the time of travel parameter for each system. The only unknown is the length of storage period (t_{sp}). With an average storage period of 183 days (half a year) only one of calculated τ values for the 204 ATES systems was larger than one; a very small system in high ambient groundwater flow velocity. On top of meeting the requirement of Ceric and Haitjema, the thermal retardation also causes the heat to flow at half the speed of water, which then makes the assumption of preservation of a cylindrical shape during displacement an acceptable simplification. These conditions allow the definition of the recovery efficiency as a function of the overlapping part of the cylinders, with and without the displacement induced by ambient groundwater flow. Assuming that the ambient groundwater flow is horizontal, the surface area of the thermal footprints before and after displacement with the groundwater flow represents this efficiency, Fig. 10 (top).

Goniometric rules are used to express the overlapping surface area ($A_{overlap}$) of the thermal footprint as a function of groundwater flow velocity and thermal radius, as follows:

$$A_{overlap} = 2{R_{th}}^2 a \cos\left(\frac{t_{sp}u_*}{2R_{th}}\right) - t_{sp}u_*\sqrt{{R_{th}}^2 - \frac{1}{4}(t_{sp}u_*)^2} \quad (10)$$

in which the velocity of the thermal front ($t_{sp}\,u_*$) is 2 times PO in Fig. 10 (top). Substituting the relation between efficiency (η_{th}), thermal footprint ($A_{footprint}$) and overlapping area:

$$A_{overlap} = \eta_{th}A_{footprint} \rightarrow A_{overlap} = \eta_{th}\pi{R_{th}}^2 \quad (11)$$

results in a relation between efficiency, flow velocity and the thermal radius;

$$\eta_{th} = \frac{2}{\pi}a \cos\left(\frac{t_{sp}u_*}{2R_{th}}\right) - \frac{t_{sp}u_*}{\pi{R_{th}}^2}\sqrt{{R_{th}}^2 - \frac{1}{4}(t_{sp}u_*)^2}. \quad (12)$$

For every ATES system with $\tau < 1$ the efficiency can be obtained with this relation. When $R_{th} > u$, the $t_{sp}\,u_*$-term under the square root contributes less than 1% to the obtained efficiency. Under these conditions, both right and left term of Eq. (12) depend on the ratio between the traveled distance and the thermal radius. So for any constant combination of u_* over R_{th}, the efficiency is the same, which allows to identify the efficiency as a function of the R_{th}/u-ratio for different storage periods, Fig. 10 (bottom). This can be used to identify minimum desired thermal radius (i.e. maximum desired screen length for a given storage volume) at a location with a given groundwater flow velocity to meet a minimal efficiency.

The derived relation is now used to assess the well design data with respect to the local ambient groundwater flow velocity, hydraulic conductivity and thickness of the aquifer. For each of the ATES systems in the dataset the R_{th}/u–value was determined, the relation given in Fig. 10 (bottom) is used to indicate lines of expected thermal efficiency only taking into account losses due to displacement caused by ambient groundwater flow, Fig. 11.

Fig. 11 shows that about 20% of the systems have an expected efficiency lower than 80% ($R_{th}/u < 1.1$). For the ATES systems with an expected efficiency lower than 80% (Table 4) the average storage volume is relatively small and the average flow velocity relatively high at 36 m/y. Although minimizing screen length reduces heat losses due to displacement, minimizing for conduction and dispersion losses require an optimal screen length for a particular storage volume.

3.2.3. Conclusion analytical analysis

In optimizing the storage geometry of ATES systems the applied length should be carefully considered. However, in both Figs. 6 and 9 it can be seen that many ATES systems with varying storage volumes have identical screen lengths, at various multiplications of 5 m. This likely relates to the fact that screen sections are supplied in 5 m sections,

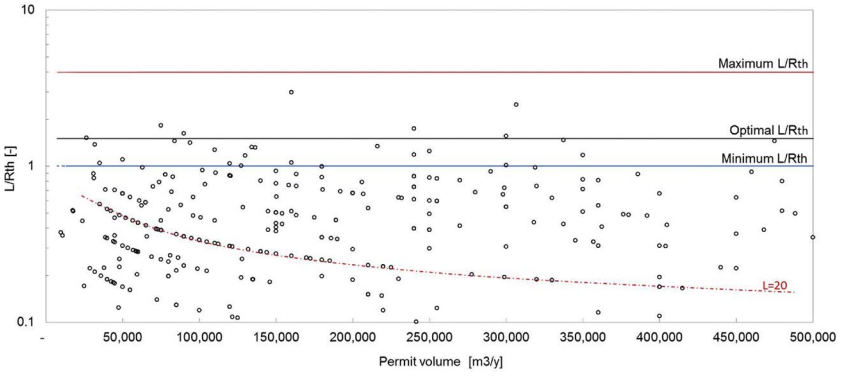

Fig. 9. L/R_{th}-value relative to permit volume of ATES systems in practice, combined with minimum ($L/R_{th} = 1$), maximum ($L/R_{th} = 4$) and optimal ($L/R_{th} = 1.5$) L/R_{th} for conduction and dispersion losses.

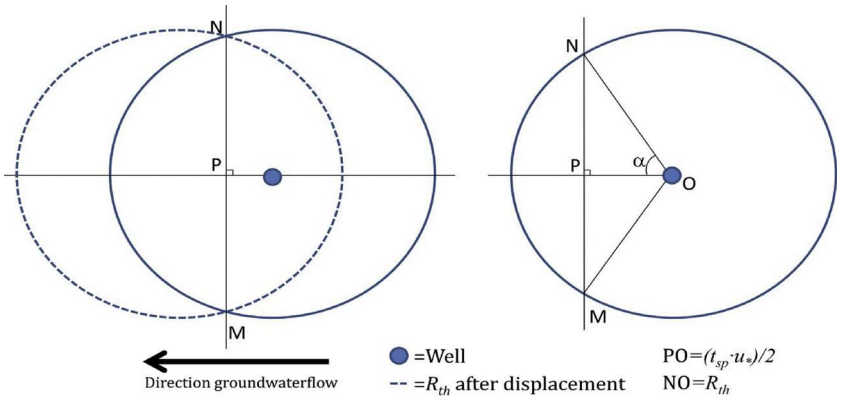

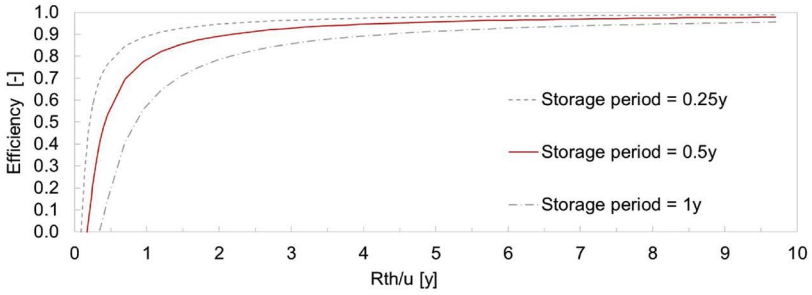

Fig. 10. Top: schematic overview of calculating the overlapping surface area of 2 identical thermal cylinders. Bottom: the derived analytical relation between losses and the thermal radius – groundwater flow velocity ratio.

which can, but are not adjusted to a specifically required length. The wide range of storage volume per single screen length (e.g. 40,000–420,000 m^3 for $L = 20$, Fig. 9) thus indicates that the screen length design indicated in the permit application are generally not based on an evaluation of storage volume and local geohydrological conditions, Dutch design standards only consider the clogging potential for ATES well design (NVOE, 2006). Particularly for smaller ATES systems, the sensitivity of recovery efficiency for screen length selection is high, as these are most vulnerable for significant losses as a consequence of ambient groundwater flow and dispersion and conduction (Figs. 8 and 10).

3.3. Numerical evaluation of energy losses

To assess the combined effect of conduction, dispersion and displacement losses, the results of the performed numerical MODFLOW simulations are discussed and compared with the straightforward and simple analytical solutions presented in the previous section. The wide range of ATES conditions for which the numerical simulations were performed resulted in recovery efficiencies between 10 and 70%. (Fig. 12).

Table 4
Results of analysis of screen length with respect to groundwater flow velocity.

	average u [m/y]	average V [m^3/y]	average R_{th} [m]
$\eta > 80\%$	6	263,000	46
$\eta < 80\%$	33	100,000	32

3.3.1. Contribution of displacement losses

The lowest efficiencies are associated with the scenarios with high ambient groundwater flow (> 50 m/year), together with relatively small thermal radius, which results in a small thermal radius over ambient groundwater flow (R_{th}/u-ratio < 1 y). For both the numerical and the analytical solution for the impact of ambient groundwater flow on recovery efficiency is very sensitive for low R_{th}/u-values. However, at higher R_{th}/u–values (> 1 y) the efficiency becomes less dependent of R_{th}/u, as dispersion and conduction losses are dominant under such conditions. In all cases the analytical solution overestimates the efficiency compared to numerical results, because the analytical solution does not take account for conduction and dispersion losses. To estimate

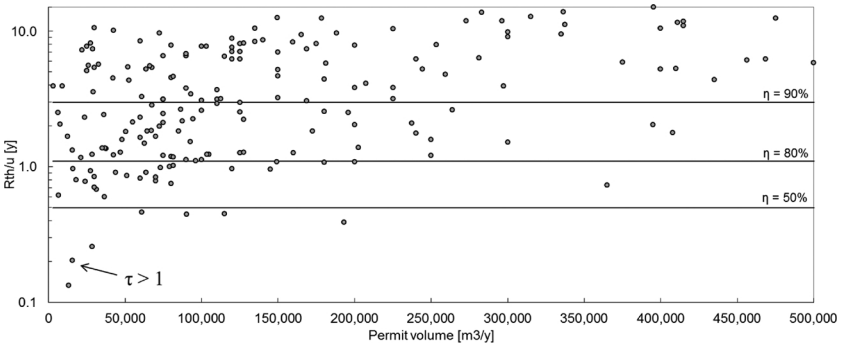

Fig. 11. R_{th}/u-values for ATES systems in the dataset with thresholds for different thermal recovery efficiencies.

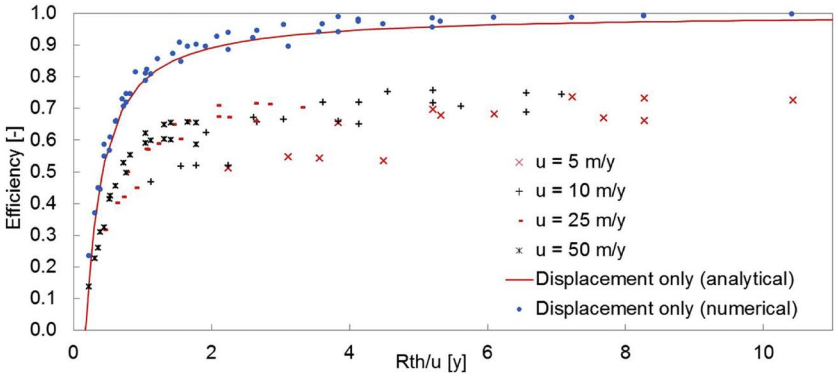

Fig. 12. Relation between efficiency and thermal radius over groundwater flow velocity (R_{th}/u) for numerical simulation results and analytical solution (Equation (12)) for a 0.5 y storage period.

the efficiency for the numerical simulations that would result under the impact of displacement only, the obtained efficiencies under no flow conditions are used as a reference (following (η_u) for $u = 5$ m/y; $\eta_5 = (1\text{-}\eta_0) + \eta_5$). These numerically derived estimates show a good resemblance with the analytical relation. This confirms that the analytical approach is valid to determine displacement losses separately.

3.3.2. Contribution of conduction and dispersion losses

Simulated efficiencies for the scenarios without ambient groundwater flow were highest, up to 75%, and highly correlated with the surface area over volume ratio A/V (Fig. 13), in contrast with the simulations with the highest ambient groundwater flow (50 m/y). Also the A/V ratios calculated for earlier simulation studies and experiments without ambient groundwater flow (Caljé, 2010; Doughty et al., 1982; Lopik et al., 2016) strongly correlate with the observed efficiencies in these studies. Like in this study, the results from Lopik et al. (2016) and Doughty et al. (1982) consist of a series systematic changing boundary conditions which allows for verification of the relations found in Fig. 13. Results of both Lopik et al. (2016) and Doughty et al. (1982) show a linear relation with similar slope between the surface area over volume ratio (A/V) and efficiency in the absence of ambient groundwater flow. The excellent correlation efficiency with the A/V ratio for each study with no ambient groundwater flow, indicates that under similar condition the efficiency of ATES systems for a particular aquifer system and operational mode can be interpolated based on A/V.

Although similar, the efficiencies at a particular A/V ratio deviate for these different modeling studies and are likely to be caused by small differences in parameters and model set-up. E.g.; both Doughty et al. (1982) and Lopik et al. (2016) used an axisymmetric model and a finer vertical spatial discretization compared to this study, resulting in differences in numerical dispersion. Also, Doughty et al. (1982) uses no dispersion, which explains why their simulations show the highest efficiency. Lopik et al. (2016) uses shorter and less storage cycles as well as a slightly smaller dispersion coefficients compared to this study. From these (small) differences can be seen that at simulations with higher dispersion, the A/V – efficiency relation becomes steeper, small systems which have a larger A/V ratio then suffer relatively more, confirming the earlier observation from Fig. 7 that at larger storage volumes conduction losses dominate.

3.3.3. Combined displacement and conduction & dispersion losses

As found by Doughty et al. (1982) the optimum for L/R_{th} ratio for a particular ATES storage volume is around 1.5 in the absence of ambient groundwater flow. However this optimal ratio shifts to lower values with increasing ambient groundwater flow velocity (Fig. 14). The optima remains flat for higher groundwater flow velocity, only for the smallest system (12,000 m^3) at the highest ambient groundwater flow (50 m/y) tested, this is not the case within the simulated conditions.

To identify the optimal L/R_{th} at different rates of groundwater flow velocity, the L/R_{th} value of the simulation series of each storage volume and groundwater flow velocity with the highest efficiency was selected from the different L/R_{th} scenarios simulated. To take into account the flat optima also the L/R_{th} values with less than 5% deviation in efficiency were selected. For each of the simulated ambient groundwater flow velocity, the average and the standard deviation of the optimal L/R_{th} values were calculated and plotted in Fig. 15. This empirical relation shows how the well design for ATES wells can be optimized taking account conduction, dispersion and displacement losses. It also shows that at higher ambient groundwater flow, well design is more critical, since the allowed deviation of the optimal solution becomes smaller. Despite the limited number of simulations (120), the number and spreading of different conditions is sufficient to use this relation in design practice.

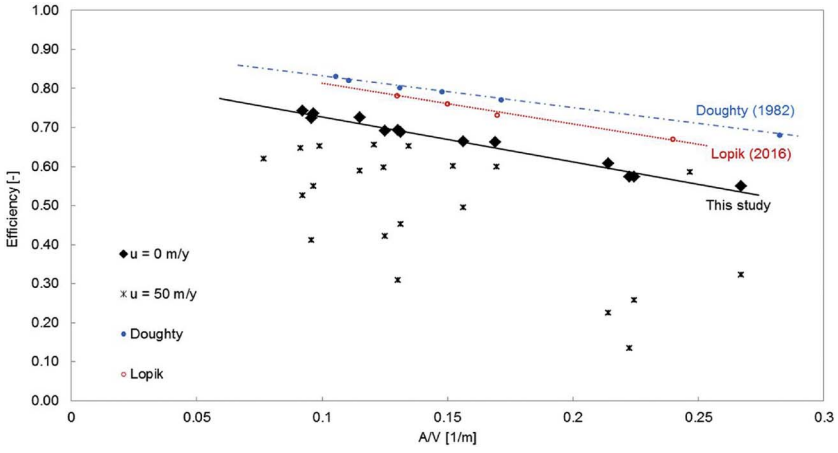

Fig. 13. Simulated efficiencies relative to geometric property (A/V) from this and other studies at u = 0 m/y and for u = 50 m/y from the simulations done in this study. The Pearson correlation between A/V and efficiency is −0,99 for u = 0 m/y. and −0.58 for u = 50 m/y. From the Lopik et al. (2016) study, only the data are used from the simulations that excluded buoyancy flow.

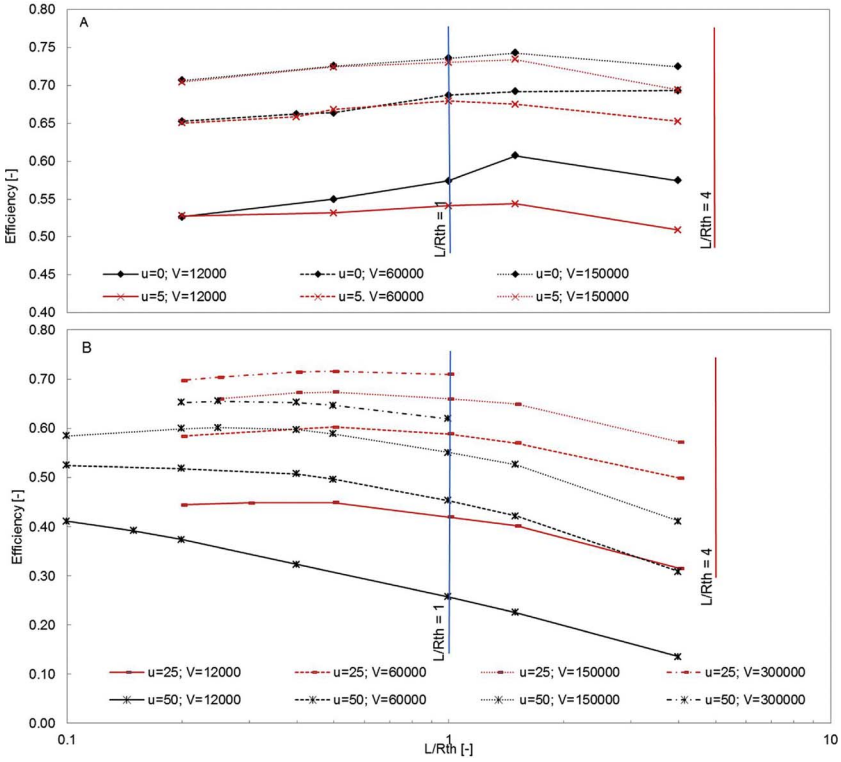

Fig. 14. Simulated efficiencies for different groundwater flows (u) and screen length over thermal Radius (L/R_{th}) of various storage volumes. A. is at no/low ambient groundwater flow (Doughty applies). B. is at high ambient groundwater flow.

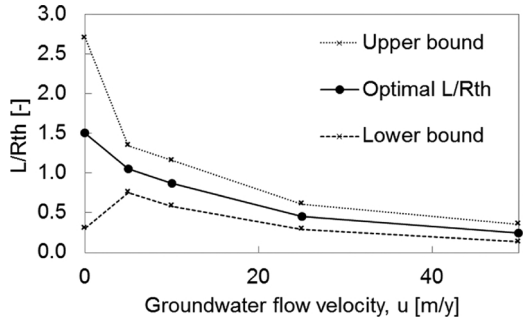

Fig. 15. Optimal L/R_{th} for different groundwater flows empirically derived from simulation results.

4. Discussion

4.1. Size and variation in seasonal storage volume

As shown in this research storage volume is an important parameter affecting recovery efficiency. In assessing this efficiency it has been assumed that the infiltrated and extracted volume is equal for each cycle. However, in practice the infiltration and extraction volume from wells are typically not equal due to variations in heating and cooling demand. This can have a significant influence on the perceived recovery efficiency per cycle. Monitoring data indicates energy imbalances varying between −22% and +15% (Willemsen, 2016). Because in general ATES systems have to meet energy balance for a certain period, in The Netherlands 3–5 years depending on provincial legislation, a representative storage volume can be used to assess conduction and displacement losses. Because the absolute losses increase with increasing storage volumes, it is more beneficial to optimize for maximum storage volume. This is also reflected in Eq. (7) where can be seen that the A/V-value has a flat optimum at larger storage volumes (Fig. 8), and also in the relation identified by Doughty et al. (1982) and shown in Fig. 14. Therefore, the permitted capacity data of the ATES wells in The Netherlands were used to compare theoretical well design approaches with field data, Fig. 9. However, in practice ATES systems deviate from their permit capacity to store heat because ATES operators request a larger permit capacity to allow for flexibility during operation; e.g. building energy demand may be higher than expected, possible future growth, change of building function and seasonal fluctuations. This influences the shape and thus the losses of the heat storage. Operational data of ATES systems from different databases have been used in

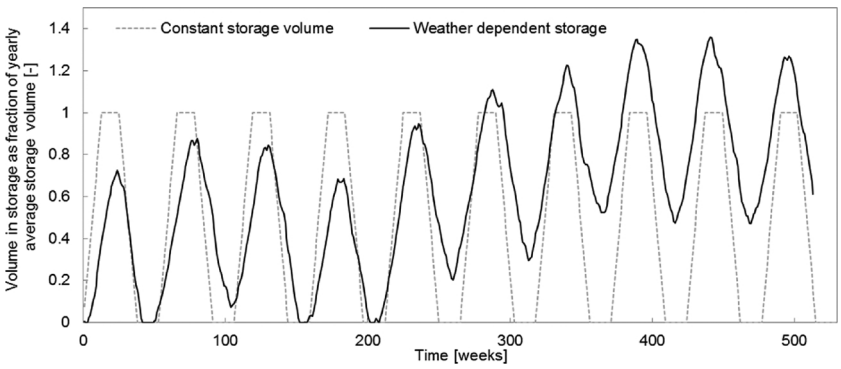

Fig. 16. Volume in storage of warm well for different energy demand patterns.

regional and national studies and evaluations (CBS, 2005; Graaf et al., 2016; SIKB, 2015b; Willemsen, 2016) all showing that ATES systems yearly actually only use 40–60% of their initially requested and permitted capacity. The ranges of systems sizes presented in this study, e.g. Figs. 5 and 6, are therefore much smaller in practice.

Also variations in seasons affect the total storage volume in the ATES wells. In this study the common assumption was made, that the average yearly volume is infiltrated and extracted during the winter and summer, with a storage period in between, resulting in a block-scheme like infiltration, storage and extraction pattern. However, heating and cooling demand typically does not balance perfectly during a year and seasonal variations may cause temporal imbalances, resulting in a sometimes smaller and sometimes larger heat storage compared to the yearly average storage. For example, heat may remain in warm wells during a couple of warm winters until a colder winter depletes the warm well. The effect of this aspect is illustrated by the presentation of the cumulative volume stored in a well relative to the average value for multiple years, Fig. 16. This pattern is derived from the storage volume variation based on the monitored and projected outside air temperature (2010–2020) of the weather station of De Bilt in The Netherlands (KNMI, 2013). The energy demand pattern is determined by deriving the energy demand for each day by scaling the yearly average energy demand to the deviation of the daily temperature from the average outside air temperature of the evaluation period. As a result of this seasonal variations imbalances occur over the years, resulting in varying stored volume in the wells. From Fig. 16 can be seen that the maximum storage capacity occurring in practice is around 150% of the average yearly storage volume. This exercise was done for different climatic datasets (monitored as wells as projections), all giving the same outcome, that the maximum storage in the well is about 150% of the average yearly storage.

The fact that well design can be best determined for maximum storage volume, then leads to the conclusion that 150% of the expected yearly average storage volume, which in turn is about 75% of the permitted capacity (50% of permitted capacity is used in practice) must be used as a basis for well design. Correcting the data of the permitted volumes for these two aspects results in the ATES systems plotted in Figs. 9 and 11 to respectively move up- and downwards.

4.2. Additional well design criteria in practice

The well design criteria required to assess and optimize the thermal recovery efficiency were considered in this study. However, in practice additional aspects such as capacity, prevention of well clogging, available aquifer thickness, mutual interaction and drilling and installation costs all play a role in determining the well design. In practice the determination of screen length is mainly based on the maximum desired pumping rate (NVOE, 2006). Together with minimizing drilling costs this is a driver for screen lengths that are too short to achieve optimal thermal efficiency, which is clearly reflected in Fig. 9. In the Netherlands, a clear guideline or method available to take account for losses as a result of ambient groundwater flow in well design is currently lacking (NVOE, 2006), which is reflected in Fig. 11. The effect of a partially penetrating well on the distribution and A/V-ratio of heat is both not discussed in this study and not taken into account in current practice. However, given the identified significant effect of the A/V-ratio on efficiency, the efficiency of a partially penetrating well may deviate significantly from a fully penetrating well with the same storage volume and screen length. For partially penetrating wells the aquifer anisotropy is also an important parameter to consider.

In this study is shown that suboptimal well design may have a large influence on well efficiency, but can also be limited relatively easily. As shown in Figs. 8 and 14, the dependency for both A/V and L/R_{th} with efficiency has a flat optimum beyond some threshold, which then allows dealing with local aquifer thickness conditions and uncertainties in storage volume now this threshold is known.

4.3. The impact of ambient groundwater flow on the efficiency of ATES systems

High ambient groundwater flow affects the recovery efficiency of ATES systems significantly. The missing framework to assess stored heat losses due to groundwater flow is introduced in this paper. Also the orientation of ATES wells with respect to the ambient flow direction needs to be taken into account. Warm and cold wells need to be oriented perpendicular to the flow direction. For individual systems this framework helps to improve well efficiency, a drawback of the presented framework is, however, the resulting large thermal radii and suboptimal use of aquifer thickness. In areas with many ATES systems close together this may lead to scarcity of subsurface space for ATES. In such busy areas with high ambient groundwater flow, planning strategies should work towards placement of same type of wells in the direction of the groundwater flow, where then only the most upstream wells will suffer from losses due to groundwater flow, for which compensation arrangements may be made. Multi doublet systems on the other hand may better use the strategy to place well of the same type in the direction of the flow and infiltrate relatively more heat in the upstream and extract more from the downstream well to compensate for the ambient groundwater flow losses, as was described by Groot (2013).

4.4. The effect of aquifer conditions

The shape of the stored heat was assumed to have a cylindrical shape in this evaluation of well design. However, in a heterogeneous aquifer the storage volume does not have the shape of a ‘perfect’ cylinder, resulting in a varying thermal radius over the depth of the screen. As a consequence of heterogeneity the A/V-ratio in practice is higher compared to the expected value for a homogeneous aquifer. Although they both use a single ATES configuration, Sommer et al. (2013) and Caljé (2010) show that the net effect of heterogeneity on efficiency is limited over multiple storage cycles and its influence is much smaller compared to the effect of A/V and ambient groundwater flow on the efficiency. Only when gravel layers are present such heterogeneity may affect efficiency significantly, and should therefore best be blinded (Caljé, 2010). Next to variations in hydraulic conductivity, also variations in salinity may affect the shape of the storage volume due to buoyancy flow due to density differences. Such aspects will affect the efficiency dependencies derived for the homogeneous and isotropic conditions evaluated in this study. Also the efficiency dependency for application of ATES in more challenging geohydrological environments will require further study.

4.5. Combined wells and mutual interaction

This study focusses on optimizing the recovery efficiency of a single ATES systems and individual wells, ATES systems however cumulate in urban areas (Bloemendal et al., 2014; Hoekstra et al., 2015) and regularly share subsurface space to store or extract heat. As a consequence, additional considerations need to be taken into account, which might lead to deviations from the design consideration presented in this research. For example, planning of subsurface space occurs based on the thermal footprint (Fig. 3) of an ATES well projected at surface level (Arcadis and Bos, 2011; Li, 2014), which then promotes the use of longer screens. From the flat optima shown in Fig. 14 it can be seen that the individual well efficiency may not have to suffer much from such additional consideration. This will allow larger number of ATES systems to be accommodated in such areas and with that the overall CO_2 emission reduce (Jaxa-Rozen et al., 2015). Also, large ATES systems often have multiple warm and cold wells which are placed together and function as one single storage in the subsurface. The length of the screens of such combined wells should therefore also be determined based on the fact that they function as one storage volume in the subsurface, disregarding this aspect gives a suboptimal A/V and amplifies

the effect of having a larger footprint, in areas where this must be prevented. From this is concluded that combining wells, also requires a well design for the individual wells based on storage capacity of both wells together. However, in such busy aquifers best would be to promote the use of the full aquifer thickness for wells and use a full 3D planning strategy.

5. Conclusion

In this study an evaluation of ATES characteristics from practice together with analytical and numerical simulations were used to develop the missing framework for ATES well design to achieve optimal recovery efficiency. This work includes the losses due to heat displacement with ambient groundwater flow. The results show that two main processes control thermal recovery efficiencies of ATES systems. These are due to the thermal energy losses that occur 1) across the boundaries of the stored volume by mainly conduction and dispersion only at smaller storage volumes and 2) due to the displacement of stored volumes by ambient groundwater flow.

For the latter process, an analytical expression was deduced that suitably describes thermal recovery efficiency as a function of the ratio of the thermal radius over ambient groundwater flow velocity (R_{th}/u). For the conditions tested, at $R_{th}/u < 1$ the displacement losses were dominant and thus would require minimization of the well screen length or maximize the volume stored. Obviously, practical aspects, such as required minimum well capacity or the availability of suitable aquifers, may prevent the use of optimal screen lengths as is illustrated for a large part (15%) of the evaluated Dutch ATES systems that indicate an a efficiency of less than 50%, due to ambient groundwater flow (Fig. 11).

With respect to the dispersion and conduction losses it was shown that conduction is dominating and for the numerical simulation results of this and previous studies, thermal recovery efficiency linearly increases with decreasing surface area over volume ratios of the stored volume (A/V) for a particular set of operational and geohydrological conditions. With respect to the losses due to conduction and dispersion, the optimal screen length has a flat optimum, which allows to also take account for other considerations in well design like neighboring systems and partially penetrating effects.

For the optimization of thermal recovery efficiency with respect to both main processes, the optimal value for the ratio of well screen length over thermal radius (L/R_{th}) decreases with increasing ambient groundwater flow velocities as well as its sensitivity for efficiency. With the insights on the controls on thermal recovery efficiency derived in this study, the assessment of suitable storage volumes, as well as the selection of suitable aquifer sections and well screen lengths, can be supported to maximize the thermal recovery of future seasonal ATES systems in sandy aquifers world-wide.

Acknowledgements

This research was supported by Climate-kic E-use (aq) and the URSES research program funded by the Dutch organization for scientific research (NWO) and Shell, grant number 408-13-030. We thank two anonymous reviewers for their valuable comments on the manuscript.

References

Anderson, M.P., 2005. Heat as a ground water tracer. Ground Water 43, 951–968.
Arcadis, T.T.E., Bos, W., 2011. Handreiking masterplannen bodemenergie. SKB, Gouda.
Bear, J., Jacobs, M., 1965. On the movement of water bodies injected into aquifers. J. Hydrol. 3, 37–57.
Bear, J., 1979. Hydraulics of Groundwater. Dover Publications Inc., Mineola, New York.
Bloemendal, M., Olsthoorn, T., Boons, F., 2014. How to achieve optimal and sustainable use of the subsurface for Aquifer Thermal Energy Storage. Energy Policy 66, 104–114.
Bloemendal, M., Olsthoorn, T., van de Ven, F., 2015. Combining climatic and geo-hydrological preconditions as a method to determine world potential for aquifer thermal energy storage. Sci. Total Environ. 538, 621–633.
Bonte, M., 2013. Imacts of Shallow Geothermal Energy on Groundwater Quality, Geo Sciences. Vrije Universiteit Amsterdam, Amsterdam.
Bonte, M., Mesman, G., Kools, S., Meerkerk, M., Schriks, M., 2013a. Effecten en risico's van gesloten bodemenergiesystemen. KWR Watercycle Research Institute, Nieuwegein.
Bonte, M., Van Breukelen, B.M., Stuyfzand, P.J., 2013b. Environmental impacts of aquifer thermal energy storage investigated by field and laboratory experiments. J. Water Clim. Change 4, 77.
CBS, 2005. In: CBS (Ed.), Hernieuwbare energie in Nederland 2004. Central Authority for Statistics in NL, Den Haag.
CBS, 2016a. In: CBS (Ed.), Issued Building Permits 1990–2015 Retrieved from Statline Database. Central authority for statistics in NL, Den Haag.
CBS, 2016b. Voorraad woningen en niet-woningen; mutaties, gebruiksfunctie, regio. CBS.nl.
Caljé, R., 2010. Future Use of Aquifer Thermal Energy Storage Inbelow the Historic Centre of Amsterdam, Hydrology. Delft University of Technology, Delft.
Ceric, A., Haitjema, H., 2005. On using Simple Time-of-travel capture zone delineation methods. Groundwater 43, 403–412.
Doughty, C., Hellstrom, G., Tsang, C.F., 1982. A dimensionless approach to the Thermal behaviour of an Aquifer Thermal Energy Storage System. Water Resour. Res. 18, 571–587.
EIA, 2009. Residential Energy Consumption Survey. US Energy Information Administation.
EU, 2010. In: In: Union O.J.o.t.E (Ed.), Directive on the Energy Performance of Buildings 153. EU-Parliament, European Union, Strasbourg, pp. 13–35.
Eugster, W.J., Sanner, B., 2007. Technological Status of Shallow Geothermal Energy in Europe. European Geothermal Congress, Unterhaching, Germany.
Fry, V.A., 2009. Lessons from London: regulation of open-loop ground source heat pumps in central London. Geol. Soc. Lond. 42, 325–334.
Gelhar, L.W., Welty, C., Rehfeldt, K.R., 1992. A critical review of data on field-scale dispersion in aquifers. Water Resour. Res. 1955–1974.
Graaf, A.D., Heijer, R., Postma, S., 2016. Evaluatie Wijzigingsbesluit bodemenergiesystemen. Buro 38 in commision of ministry of Intrastructure and environment, Cothen.
Groot, J., 2013. Optimizing Energy Storage and Reproduction for Aquifer Thermal Energy Storage Geosciences. University of Utercht.
Haehnlein, S., Bayer, P., Blum, P., 2010. International legal status of the use of shallow geothermal energy. Renew. Sustain. Energy Rev. 14, 2611–2625.
Harbaugh, A.W., Banta, E.R., Hill, M.C., McDonald, M.G., 2000. In: USGS (Ed.), Modflow-2000, The U.S. Geological Survey Modular Ground-Water Model—User Guide to Modularization Concepts and the Ground-Water Flow Process. US Geological Survey, Virginia.
Hartog, N., Drijver, B., Dinkla, I., Bonte, M., 2013. Field assessment of the impacts of Aquifer Thermal Energy Storage (ATES) systems on chemical and microbial groundwater composition. In: European Geothermal Conference. Pisa.
Hecht-Mendez, J., Molina-Giraldo, N., Blum, P., Bayer, P., 2010. Evaluating MT3DMS for heat transport simulation of closed geothermal systems. Ground Water 48, 741–756.
Hoekstra, N., Slenders, H., van de Mark, B., Smit, M., Bloemendal, M., Van de Ven, F., Andreu, A., Sani, D., Simmons, N., 2015. Europe-Wide Use of Sustainable Energy from Aquifers, Complete Report. Climate-KIC.
Jaxa-Rozen, M., Kwakkel, J.H., Bloemendal, M., 2015. The Adoption and Diffusion of Common-Pool Resource-Dependent Technologies: The Case of Aquifer Thermal Energy Storage Systems. PICMET, Portland.
KNMI, 2013. Hourly data 1980-2010, Climatic Projections KNMI W+ Scenario 2010–2045 for Weather Station 260, de Bilt.
Kasenow, M., 2002. Determination of Hydraulic Conductiviy from Grain Size Anaysis. Water Resources Publications LLC, Highlands Ranch, Colorado.
Kim, J., Lee, Y., Yoon, W.S., Jeon, J.S., Koo, M.-H., Keehm, Y., 2010. Numerical modeling of aquifer thermal energy storage system. Energy 35, 4955–4965.
LGR, 2012. In: Netherlands P.o.T (Ed.), Dutch Register/Database for Groundwater Abstractions.
Li, Q., 2014. Optimal Use of the Subsurface for ATES Systems in Busy Areas Hydrology. Delft University of Technology.
Lopik, J.H.V., Hartog, N., Zaadnoordijk, W.J., 2016. The use of salinity contrast for density difference compensation to improve the thermal recovery efficiency in high-temperature aquifer thermal energy storage systems. Hydrogeol. J. 24 (5), 1255–1271. http://dx.doi.org/10.1007/s10040-016-1366-2.
Ministry-of-Internal-Affairs, 2012. Bouwbesluit (Building Act). Ministry-of-Internal-Affairs, Den Haag.
Molz, F.J., Warman, J.C., Jones, T.E., 1978. Aquifer storage of heated water. Groundwater 16.
Molz, F.J., Melville, J.G., Parr, D.D., King, D.A., Hopf, M.T., 1983. Aquifer thermal energy storage' a well doublet experiment at increased temperatures. Ground Water 19, 149–160.
NVOE, 2006. Richtlijnen Ondergrondse Energieopslag, Design Guidelines of Dutch Branche Association for Geothermal Energy Storage. Woerden.
Nagano, K., Mochida, T., Ochifuji, K., 2002. Influence of natural convection on forced horizontal flow in saturated porous media for aquifer thermal energy storage. Appl. Therm. Eng. 22, 1299–1311.
Réveillère, A., Hamm, V., Lesueur, H., Cordier, E., Goblet, P., 2013. Geothermal contribution to the energy mix of a heating network when using Aquifer Thermal Energy Storage: modeling and application to the Paris basin. Geothermics 47, 69–79.
RHC, 2013. Strategic Research and Innovation Agenda for Renewable Heating & Cooling. Renewable Heating & Cooling, European Technology Platform, Brussels.

SER, 2013. Energie Akkoord. Social Economical Counsil.
SIKB, 2015a. BRL 2100 Mechnisch boren. SIKB, Gouda.
SIKB, 2015b. In: NL d.p.i (Ed.), Userdata of ATES Systems, Recieved from 4 provinces of the Netherlands in 2015, Gouda.
Sommer, W., Valstar, J., van Gaans, P., Grotenhuis, T., Rijnaarts, H., 2013. The impact of aquifer heterogeneity on the performance of aquifer thermal energy storage. Water Resour. Res. 49, 8128–8138.
Sommer, W.T., Doornenbal, P.J., Drijver, B.C., van Gaans, P.F.M., Leusbrock, I., Grotenhuis, J.T.C., Rijnaarts, H.H.M., 2014. Thermal performance and heat transport in aquifer thermal energy storage. Hydrogeol. J. 22, 263–279.
Sommer, W., 2015. Modelling and Monitoring Aquifer Thermal Energy Storage. Wageningen University, Wageningen.
TNO, 2002. Boringen uit Dinoloket, digitale grondwaterkaart, Utrecht.
TNO, 2002. REGIS, Utrecht.
Tsang, C.F., 1978. Aquifer thermal energy storage. Institute of Gas Technology Symposium on Advanced Technologies for Storing Energy.
UN, 2015. Adoption of the Paris Agreement. United Nations, Framework Convention on Climate Change, Paris.
Visser, P.W., Kooi, H., Stuyfzand, P.J., 2015. The thermal impact of aquifer thermal energy storage (ATES) systems: a case study in the Netherlands, combining monitoring and modeling. Hydrogeol. J. 23, 507–532.
Willemsen, N., 2016. Rapportage bodemenergiesystemen in Nederland. RVO/IF Technology, Arnhem.
Zeghici, R.M., Oude Essink, G.H.P., Hartog, N., Sommer, W., 2015. Integrated assessment of variable density–viscosity groundwater flow for a high temperature mono-well aquifer thermal energy storage (HT-ATES) system in a geothermal reservoir. Geothermics 55, 58–68.
Zheng, C., Wang, P.P., 1999. MT3DMS: A Modular Three-Dimensional Multispecies Transport Model for Simulation of Advection, Dispersion, and Chemical Reactions of Contaminants in Groundwater Systems; Documentation and User's Guide.
Zuurbier, K.G., Hartog, N., Valstar, J., Post, V.E., van Breukelen, B.M., 2013. The impact of low-temperature seasonal aquifer thermal energy storage (SATES) systems on chlorinated solvent contaminated groundwater: modeling of spreading and degradation. J. Contam. Hydrol. 147, 1–13.